Tellus (2006), 58B, 376–389
Printed in Singapore. All rights reserved

TELLUS

Anthropogenic CO_2 in the oceans estimated using transit time distributions

By D. W. WAUGH[1*], T. M. HALL[2], B. I. McNEIL[3], R. KEY[4] and R. J. MATEAR[5],
[1]*Department of Earth and Planetary Sciences, Johns Hopkins University, Baltimore, MD 21218, USA;* [2]*NASA Goddard Institute for Space Studies, New York, NY 10025, USA;* [3]*School of Mathematics, University of New South Wales, Sydney, NSW 2052, Australia;* [4]*Geophysical Fluid Dynamics Laboratory, Princeton, NJ 08540, USA;* [5]*CSIRO Divsion of Marine Research, Hobart, TAS 7001, Australia*

(Manuscript received 12 January 2006; in final form 10 July 2006)

ABSTRACT

The distribution of anthropogenic carbon (C_{ant}) in the oceans is estimated using the transit time distribution (TTD) method applied to global measurements of chlorofluorocarbon-12 (CFC12). Unlike most other inference methods, the TTD method does not assume a single ventilation time and avoids the large uncertainty incurred by attempts to correct for the large natural carbon background in dissolved inorganic carbon measurements. The highest concentrations and deepest penetration of anthropogenic carbon are found in the North Atlantic and Southern Oceans. The estimated total inventory in 1994 is 134 Pg-C. To evaluate uncertainties the TTD method is applied to output from an ocean general circulation model (OGCM) and compared the results to the directly simulated C_{ant}. Outside of the Southern Ocean the predicted C_{ant} closely matches the directly simulated distribution, but in the Southern Ocean the TTD concentrations are biased high due to the assumption of 'constant disequilibrium'. The net result is a TTD overestimate of the global inventory by about 20%. Accounting for this bias and other centred uncertainties, an inventory range of 94–121 Pg-C is obtained. This agrees with the inventory of Sabine et al., who applied the ΔC^* method to the same data. There are, however, significant differences in the spatial distributions: The TTD estimates are smaller than ΔC^* in the upper ocean and larger at depth, consistent with biases expected in ΔC^* given its assumption of a single parcel ventilation time.

1. Introduction

Quantifying the distribution and uptake of anthropogenic carbon in the oceans is a crucial component of understanding the global carbon cycle (Houghton et al., 2001) Accordingly there has been considerable research in this area, including global measurement campaigns [e.g. World Ocean Circulation Experiment (WOCE) and the Joint Global Ocean Flux Study (JGOFS)] and the development of several different indirect methods to estimate the total accumulation of anthropogenic carbon (C_{ant}) (e.g. Brewer, 1978; Chen and Millero, 1979; Gruber et al., 1996; Goyet et al., 1999; Hall et al., 2002; Touratier and Goyet, 2004) or decadal uptake (e.g. Wallace, 1995; McNeil et al., 2003; Friis et al., 2005) from these measurements. However, there still remains large uncertainties in the estimates of ocean C_{ant}. Several assumptions are made in the inference methods, which introduce biases of uncertain magnitude. Comparisons of C_{ant} estimates from different methods have shown some substantial differences (e.g. Wanninkhof et al., 1999; Coatanoan et al., 2001; Sabine and Feely 2001; Hall et al., 2004; LoMonaco et al., 2005b), but have generally been unable to explain these discrepancies or to identify which methods are superior.

In recent years estimates from the ΔC^* method of Gruber et al., (1996) have received the greatest attention. In this method one constructs a quasi-conservative carbon tracer, C^*, from measurements of dissolved inorganic carbon (DIC) and other species by using stoichiometric ratios (Redfield ratios), assumed to be constant and uniform. Estimates of the pre-industrial C^* are then subtracted, leaving the anthropogenic component as a small residual. The ΔC^* method has been applied to data from all three major basins (Gruber, 1998; Sabine et al., 1999; Sabine et al., 2002; Lee et al., 2003) to form a global estimate of the inventory of C_{ant} (Sabine et al., 2004). These estimates of ocean C_{ant} have also been used to evaluate models (Orr et al., 2001; Matsumoto et al., 2004) and to infer air–sea fluxes of CO_2 (Gloor et al., 2003; Mikaloff Fletcher et al., 2006). However, there are many uncertainties in the ΔC^* method. Different implementations of the method can yield different results (e.g. Wanninkhof et al., 1999; LoMonaco et al., 2005b) and there are potential biases due to the assumptions of a single ventilation time, constant disequilibrium

*Corresponding author.
e-mail: waugh@jhu
DOI: 10.1111/j.1600-0889.2006.00222.x

(Hall et al., 2004; Matsumoto and Gruber, 2005), and constant and uniform Redfield ratios.

Here we estimate the distribution of anthropogenic carbon (C_{ant}) in the oceans using the transit time distribution (TTD) method (Hall et al., 2002). This method avoids the assumption of a single ventilation time and exploits a purely anthropogenic tracer (chlorofluocarbon-12, CFC12). The TTD method does not use DIC measurements and has the advantage that it avoids the large uncertainty in back-calculation methods that attempt to correct for the large natural carbon background in the DIC measurements. Hall et al. (2004) used a volume-based version of the TTD method to estimate C_{ant} in the Indian Ocean, while Waugh et al. (2004) applied a pointwise version to the subpolar North Atlantic Ocean. Here, we use the implementation of Waugh et al. (2004), which only requires measurements of temperature, salinity and CFC-12, and apply the method to the Global Data Analysis Project (GLODAP) data set (Key et al., 2004). This enables the global distribution and total inventory of C_{ant} to be estimated.

The uncertainties and potential biases in the TTD approach are evaluated by applying the method to output from an ocean general circulation model (OGCM) and comparing the results to the directly simulated C_{ant}. The TTD estimates of the C_{ant} distribution are also compared with the distribution obtained by Sabine et al. (2004) using the ΔC^* method applied to the same data set. When biases and uncertainties in the methods are taken into account there is agreement in the inventories from the two methods. There are, however, significant differences in the spatial distributions.

2. TTD Method

All observationally based methodologies to infer anthropogenic carbon make the assumption that C_{ant} penetrates the ocean as a passive, inert tracer responding to an evolving history in surface waters. The basis of the TTD method is to fully exploit this assumption in order to relax other assumptions. The concentration, $\boldsymbol{c(r, t)}$, of any passive, inert tracer at an interior point $\boldsymbol{r}$ is related to the concentration history, $c_0(t)$, on surface waters as

$$c(\mathbf{r}, t) = \int_0^\infty c_0(t - t')\mathrm{G}(\mathbf{r}, t')dt', \tag{1}$$

where $\mathrm{G}(\mathbf{r}, t)$ is the TTD at location $\mathbf{r}$ (Hall and Plumb, 1994; Haine and Hall, 2002). Eq. (1) can be applied to anthropogenic carbon if three assumptions are made. First, increasing carbon levels have not caused changes in the biological uptake of carbon. As CO_2 is not a limiting factor in the marine biosphere, this is a reasonable assumption and is widely made in estimating C_{ant}. Second, the circulation is in steady (time-averaged) state. Again this is assumption is made in other methods, including the ΔC^* method. Finally, a single surface source region dominates the water at r, so that $c_0(t)$ has no spatial dependence for given r. The implications of this assumption are discussed further below.

To apply eq. (1) it is necessary to know the surface history of C_{ant}. This is estimated using equilibrium inorganic carbon chemistry, that is, $C_{ant,0}(t) = C_{eq}(T,S,Alk^0, pCO_2(t))$-$C_{eq}(T,S,Alk^0,pCO_2 = 280$ ppm), where C_{eq} is the DIC, T the temperature, S the salinity, Alk^0 the preformed alkalinity and $pCO_2(t)$ the partial pressure of atmospheric CO_2 at time t (280ppm is taken as the pre-industrial pCO_2). C_{eq} is calculated using the standard equilibrium marine carbonate system, with the preformed alkalinity Alk^0 determined using an empirical relationship with salinity (Brewer et al., 1986), the carbonate constants from Dickson and Millero (1987) refit of Merbach et al. (1973), and atmospheric CO_2 time-series from Hansen et al. (www.giss.nasa.gov/data/si2000/ghgases). We use the Brewer et al. (1986) Alk^0 relationship rather than more recent estimates from Sabine et al. (1999) and Lee et al. (2003) as the Brewer et al. relationship depends only on salinity and not also on oxygen and nitrate or phosphate. This means only T and S measurements are required to calculate $C_{ant,0}(t)$.

It is also necessary to know the TTDs at each interior location to apply eq. (1). To calculate TTDs from tracers we make the additional assumption, as in Waugh et al. (2004), that the TTDs can be approximated by inverse Gaussian functions, that is,

$$\mathrm{G}(t) = \sqrt{\frac{\Gamma^3}{4\pi\Delta^2 t^3}}\exp\left(\frac{-\Gamma(t-\Gamma)^2}{4\Delta^2 t}\right), \tag{2}$$

where $\Gamma = \int_0^\infty \xi\mathrm{G}(\xi)d\xi$ is the mean transit time ('mean age') and $\Delta^2 = \frac{1}{2}\int_0^\infty(\xi - \Gamma)^2\mathrm{G}(\xi)d\xi$ defines the width Δ of the TTD. Given Γ and Δ it is possible to determine C_{ant} using eqs. (1) and (2), with $C_{ant,0}$ calculated as above. This is illustrated in Fig. 1(a) which shows C_{ant} variation with Γ and Δ for a water mass with $T = 10\,^\circ$ C and S = 35 psu.

The TTD parameters Γ and Δ are determined at each location using CFC12 measurements. A given CFC12 concentration can be reproduced using the convolution (1) with the observed CFC surface history (Walker et al., 2000) and TTD given by eq. (2). The variation of CFC12 with Γ and Δ is also shown in Fig. 1(a). There is a wide range of (Γ, Δ) pairs, and hence TTDs, that produce the same CFC12 concentration. This is illustrated in Fig. 1(c) which shows several TTDs that produce the same CFC12 concentration (0.22 pmol/kg, for $T = 10\,^\circ$C and S = 35 psu). The values of the ratio of width to mean age Δ/Γ of these TTDs varies from 0 to 1.5. The ratio Δ/Γ is a measure of the breadth of the TTD and the relative importance of mixing, with $\Delta/\Gamma = 0$ corresponding to purely advective flow and increasing Δ/Γ corresponding to increasing mixing. Note, here mixing is used in a very general sense, and includes diapyncal and convective mixing as well as isopycnal stirring by temporal and spatially varying eddies.

Each of the TTDs in Fig. 1(c) produce the same CFC12 concentration but produce different C_{ant} values. This is illustrated in Fig. 1(d) which shows that variation of C_{ant} with Δ/Γ, where for each Δ/Γ the value of Δ and Γ are chosen so that CFC12=0.22 pmol/kg (with $T = 10\,^\circ$C and S = 35 psu). As Δ/Γ increases the

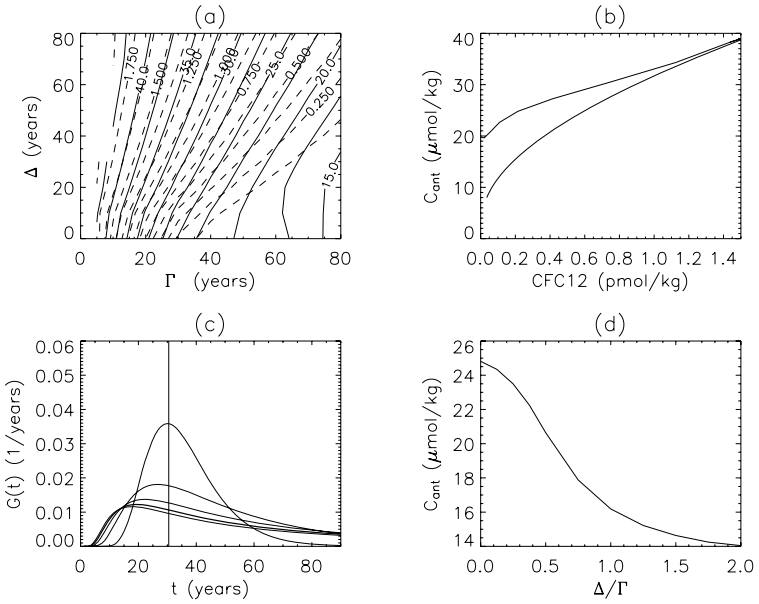

Fig. 1. (a) Variation of C_{ant} (solid; μmol/kg) and CFC12 (dashed; pmol/kg) with Γ and Δ, for a water mass with T = 10 °C and S=35 psu. (b) Relationship between C_{ant} and CFC12 for TTDs with $\Delta/\Gamma = 0$ (upper curve) and 1 (lower curve). (c) TTDs that produce a CFC12 concentration of 0.5 pmol/kg for same T and S. The value of Δ/Γ for the TTDs equal 0 (delta-function at 30 yrs), 0.5, . . . , 1.5. (d) Variation of C_{ant} with Δ/Γ for TTDs that produce the same CFC12 as in (c).

value of C_{ant} decreases, with the largest change in C_{ant} for Δ/Γ increasing from 0.2 to 0.8. Figure 1(d) illustrates that a single value of CFC12 can only limit C_{ant} to a range of values.

In principle measurements of two transient tracers with distinct histories (e.g. a CFC and bomb tritium) fix a unique (Γ, Δ) pair and, hence, a unique C_{ant}, within observational uncertainty (Waugh et al., 2002, 2004). In practice two distinct tracers are often not available simultaneously. In times and regions where they are Waugh et al. (2004) found that the tracer distributions could be well described using TTDs with the ratio $\Delta/\Gamma = 1$. Hall et al. (2004) found that CFC11 and CFC12 have histories that are too similar to put a lower bound on Δ/Γ, but that values much greater than unity could be ruled out. In fact, for estimation of C_{ant} there is little sensitivity to Δ/Γ for values less than order one. It is only the upper bound that is important to establish.

Here, we assume that $\Delta/\Gamma = 1$. The concentration of the single tracer CFC12 is then enough to completely specify the TTD and, by the convolution (1), C_{ant} . Figure 1(b) shows the variation of C_{ant} with CFC12 concentration (for water with T = 10 °C and S = 35 psu), for $\Delta = 0$ (upper curve) and $\Delta/\Gamma = 1$ (lower curve). For high CFC concentrations (young waters) there is no sensitivity to Δ/Γ (mixing), but as the CFC12 concentration decreases (older water) the value of C_{ant} for $\Delta/\Gamma = 1$ is much smaller than the no mixing limit. This can also be seen in Fig. 1(a), where the CFC12 and C_{ant} contours are parallel for small Γ, but not for large Γ.

In summary, our procedure to calculate C_{ant} at a given location is

(1) Calculate $C_{ant,0}$(t) using equilibrium inorganic carbon chemistry and observed T and S.

(2) For specified Δ/Γ determine Γ, and hence $G(t)$, for which observed CFC12 is reproduced using (1) and (2).

(3) Substitute $c_0 = C_{ant,0}$ and $G(t)$ into convolution integral (1) to determine C_{ant}.

As discussed below TTDs with $\Delta = \Gamma$ reproduce observed relationships between a suite of transient tracers. To provide an estimate of the sensitivity of the C_{ant} calculations to Δ/Γ we also consider calculations with $\Delta/\Gamma = 0.75$, and 1.25 as well as calculations with $\Delta = 0$. The $\Delta = 0$ calculations correspond to assuming there is no mixing and are equivalent to calculations using the pCFC12 age to propagate the surface C_{ant} into the interior (e.g. Thomas and Ittekkot, 2001). Comparison of these 'pCFC age' calculations with the TTD calculations reveal the regions where CFC-age calculations cannot adequately represent the effects of mixing on C_{ant}. Where the two calculations agree, CFC12 and C_{ant} have the same dependency on advection and mixing, and CFC12 may be used directly as a proxy for C_{ant}.

Several assumptions are made in the TTD method described above.

Steady-state transport: As discussed above, we assume steady-state transport when using eq. (1) to calculate C_{ant}. Modeling studies indicate that secular change due to global warming alters the carbon uptake by only around 1% (McNeil et al., 2003). However, Keeling (2005) argued for a larger effect of around 7 Pg-C due to changes driven by ocean warming and changes in the ocean circulation, although such a large effect was disputed by Sabine and Gruber (2005).

Assumed form of TTD: In the procedure outlined above we assume a specific value of Δ/Γ. Analysis of tracer measurements in the Atlantic, Indian and Pacific oceans show that the $\Delta = 0$ limit is not realistic (e.g. Hall et al., 2004; Mecking et al., 2004; Waugh et al., 2004). Furthermore, Waugh et al. (2004) and Hall et al. (2004) found that inverse Gaussian TTDs with $\Delta/\Gamma = 1$

were able to reproduce the observed relationships between transient tracer measurements in the North Atlantic subpolar gyre and Indian Ocean, respectively. This is also found in (unpublished) analysis of measurements of SF_6 and CFCs in the North and South Atlantic, suggesting that this result is general.

Although the exact value of Δ/Γ can generally not be determined there is only weak sensitivity of C_{ant} to Δ/Γ for moderate and larger mixing ($\Delta/\Gamma \geq 0.75$). For example, in the case shown in Fig. 1(d) $C_{ant} = 16.5 \pm 1.5 \mu$mol/kg for $\Delta/\Gamma = 1 \pm 0.25$. Similar sensitivity is found in the analysis of Waugh et al. (2004) and below.

Single dominant water-mass source: We have not yet quantified the error incurred by this assumption. It will be largest where different water masses with very different $C_{ant,0}$ (due to different T and S) mix in comparable proportions. In this case, however, the waters are likely to be old, because they are far from either source and the fractional C_{ant} error may be large, but the absolute C_{ant} concentrations will be small. Moreover, the error can be positive or negative, and, therefore, will tend to cancel when calculating inventories over a large scale.

CFC saturation: We assume CFC12 to be 100% saturated in surface waters when determining Γ and Δ. If the true saturation is less, then our estimated TTD will to be too old. As a result, too little C_{ant} to be propagated into the interior.

Constant disequilibrium: In the above calculation of $C_{ant,0}(t)$ we have neglected, as in ΔC^* and most other studies, the evolution of the air–sea CO_2 disequilibrium in our estimates, that is, we assume the disequilibrium is constant in time (but not in space). If, however, C_{ant} in surface waters does not keep pace with the exponential growth in atmospheric CO_2 then assuming that it does leads to an overestimate of C_{ant}. Hall et al. (2004) relaxed this assumption using a volume-integrated TTD method and obtained a 6% to 9% reduction in C_{ant} uptake in the Indian Ocean. Unfortunately, their methodology cannot easily be applied globally.

The final two assumptions are equivalent to assuming that the CFC equilibration can be used to estimate CO_2 equilibration. The errors resulting from the two assumptions at least partially cancel. In regions where CFC12 is undersaturated at the surface C_{ant} is likely also undersaturated, so the underestimate of C_{ant} due to assuming 100% CFC saturation is counteracted by the overestimate due to the assumption of constant disequilibrium for CO_2. The largest error is expected when the saturation of surface C_{ant} is much less than that of surface CFC12, and in this case our method will overestimate the interior C_{ant}.

3. TTD Calculations

We apply the TTD calculations described above to the GLODAP v1.1 hydrographic and CFC data (Key et al., 2004). These are the data used by Sabine et al. (2004). There exist locations that have CFC measurements but for which ΔC^* estimates of C_{ant} do not exist (because of lack of DIC measurements). Although the TTD method can be applied to these locations we perform TTD calculations only for locations for which ΔC^* estimates are available so that the same measurements go into the comparisons between the two methods. As in the ΔC^* calculations, C_{ant} is calculated for the date of the measurements (which varies between 1990 and 1998) and no account is made of the time differences of the C_{ant} estimates when forming regional averages or global column-inventory maps. Regional averages or column inventories, therefore, represent values for average year of the data (1994).

3.1. Regional Distributions

We first examine vertical profiles of the average C_{ant} for different regions. The thick solid curves in Fig. 2 show the regional-average C_{ant} from TTD calculations using $\Delta = \Gamma$. (These profiles were formed by averaging all data within 250 m intervals and the specified regions, with no areal weighting.) These estimates show C_{ant} values around 40–50 μmol/kg at the surface, with a rapid decrease in the upper 1000 to 1500 m. In most regions C_{ant} is approximately constant with depth below 2000 m, but the deep-water value varies between basins. In the Indian and Pacific Oceans $C_{ant} \sim 2.5$ μmol/kg below 2000 m, compared with $C_{ant} \sim 5$ μmol/kg in the tropical Atlantic Ocean and $C_{ant} \sim 10$ μmol/kg in the Southern Ocean. The value of C_{ant} below 2000 m is, however, not constant in the South and North Atlantic oceans. In the South Atlantic there is a local minimum around 3000 m with increased C_{ant} at the bottom, while there is a gradual decrease in C_{ant} in the North Atlantic from 20 μmol/kg around 1500 m to around 7 μmol/kg at 5000 m.

The CFC instrumental detection limit is about 0.005 pmol/kg. This value occurs nearly uniformly in the Indian and Pacific Oceans below 200 m depth, indicating that in these regions CFC12 is at or below the detection limit. Strict application of the TTD method to a CFC12 concentration of 0.005 pmol/kg yield $C_{ant} \approx 2.5$ μmol/kg, in 1994 for $\Delta/\Gamma = 1$ and typical T and S. As the true C_{ant} might be much smaller integrating these 'detection-limit' C_{ant} concentrations to form an inventory causes a positive bias. We correct for this conservatively when calculating inventories by assuming C_{ant} to be zero if $C_{ant} \leq 2.5$ μmol/kg. The effect on the inventory is relatively small compared to other uncertainties (see below).

In the above TTD calculations we have assumed that the TTDs are broad, that is, there is significant mixing. To examine the impact of this mixing on estimates of C_{ant} from CFC measurements we now compare the TTD estimates with those from $\Delta = 0$ (pCFC age) calculations. As shown in Fig. 2 the TTD and pCFC age estimates (thick solid and dotted curves) agreement in the upper 500–700 m, indicating that in upper waters CFC12 can be used as a proxy for C_{ant} without consideration of mixing. However, for deeper waters there are significant differences, with the TTD estimate 10–15 μmol/kg less than that assuming no mixing. This difference occurs because over

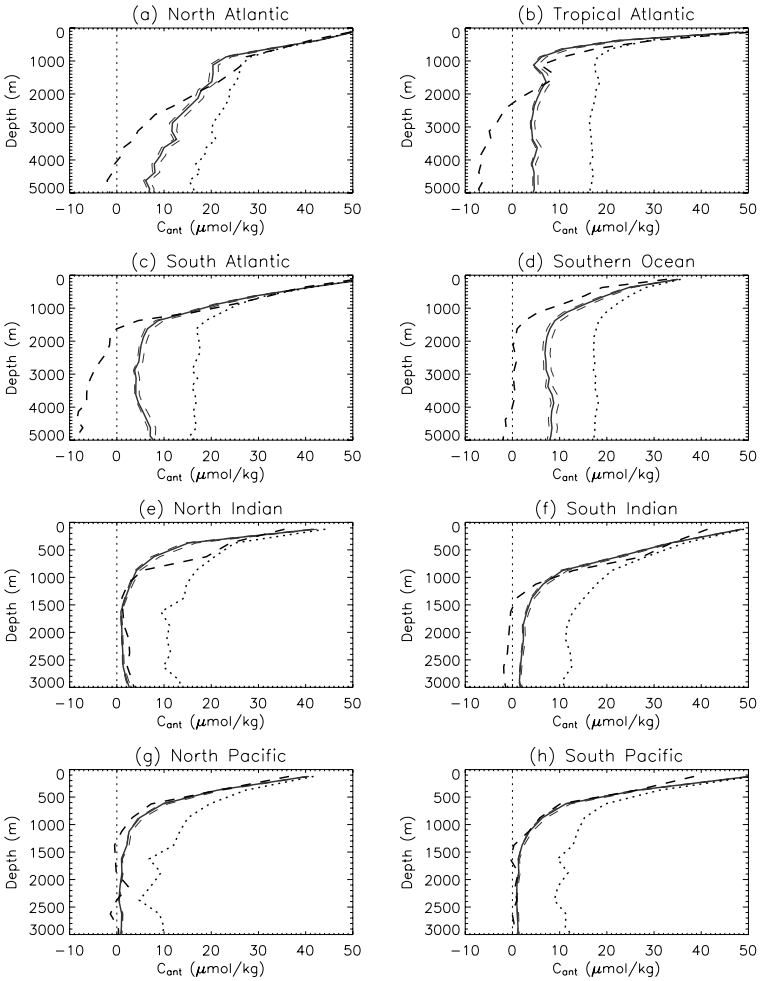

Fig. 2. Comparison of regional average C_{ant} from ΔC^* (dashed curves), TTD (thick solid) and pCFC age (dotted) methods. Thin curves show C_{ant} from TTD with $\Delta/\Gamma =$ 0.75 and 1.25. (a) North Atlantic (20–70 N), (b) Tropical Atlantic (20 S to 20 N), (c) South Atlantic (40 to 20 S), (d) Southern Ocean (0–360 E, 70 to 50 S), (e) North Indian (0–30 N), (f) South Indian (40S to 0), (g) North Pacific (0–60 N) and (h) South Pacific (40S to 0).

the time history relevant for these waters the CFC12 history is more non-linear than surface C_{ant} and the CFC12 ages preferentially weigh young components of broad TTDs. Using the CFC12 age rather than the whole TTD one then looks too recently in the surface C_{ant} history and overestimates C_{ant} (Hall et al., 2002).

3.2. Column Inventories

We now consider the vertically integrated (column) C_{ant} inventories. To calculate column and global inventories the individual sample estimates were objectively mapped onto a 1 degree grid with 33 levels, with intervals ranging from 10 m near the surface to 500 m below 2000 m. This is the same mapping as used by Sabine et al. (2004).

Figure 3(a) shows the global map of column C_{ant} from the TTD calculations. There is a large range of values (10 to 90 mol/m^2), with significant inter-ocean differences. High values are found in the North Atlantic and southern high latitudes where deep water is formed, and low values occur in the Northern Indian and Pacific Oceans. Although the highest column values occur in the Atlantic basin, the Pacific basin has a larger total inventory because of its larger volume, see Table 1. Also, the Southern Hemisphere inventory exceeds that of the Northern Hemisphere. As shown in previous sections, the C_{ant} concentration decays rapidly with depth. As a result the majority of the total inventory comes from upper waters: around 50% occurs in the upper 500 m and 75% in the upper 1500 m.

Table 1. Distribution of C_{ant} inventories, in Pg-C, by basin and latitude band

	Atlantic	Pacific	Indian	World
50°–65° N	4	1	–	5 (4%)
14°–50° N	17	12	1	30 (22%)
14° S–14° N	8	11	4	23 (17%)
50°–14° S	15	23	17	55 (40%)
-50° S	5	10	6	21 (16%)
total	49 (37%)	57 (42%)	28 (21%)	134

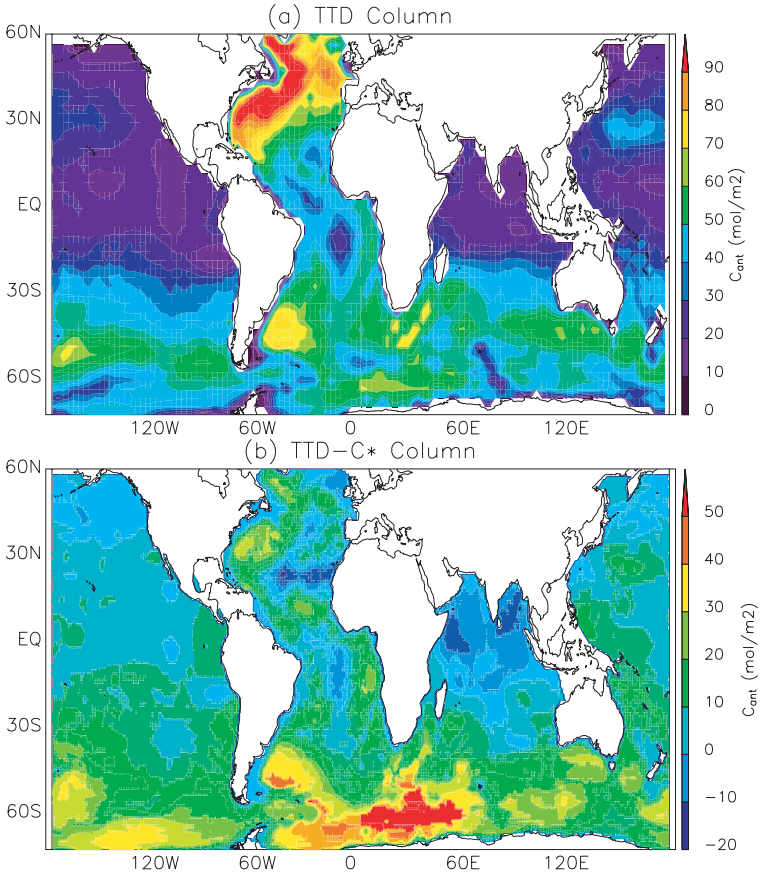

Fig. 3. Global map of (a) column C_{ant} from TTD calculations, and (b) difference between TTD and ΔC^* estimates from Sabine et al. (2004).

The total inventory from these calculations is 134 Pg-C. The GLODAP data does not include data from marginal seas or from the Arctic Ocean. To account for these regions Sabine et al. (2004) added 12 Pg-C to their estimates to obtain a global inventory. Doing the same to our calculations results in a global inventory of 146 Pg-C. However, in this paper, unless otherwise stated, when we refer to the total inventory we are referring to the total inventory of the regions covered by the GLODAP data set, and do not include marginal seas or the Arctic Ocean.

As discussed in Section 4, there is a positive bias in the TTD estimates for deep waters with CFC12 near or below the measurement detection limit. For CFC12 ~ 0.005 pmol/kg (and typical deep water values of T and S) the TTD calculation yields C_{ant} (for 1994) around 2.5 μmol/kg. To account for this bias, in the calculation of column inventories shown in Fig. 3(a) we set $C_{ant} = 0$ in any grid boxes with $C_{ant} \leq 2.5$ μmol/kg. This occurs only north of 40 S in Indian and Pacific oceans, and in small regions in central midlatitudes (20–40 degrees) of North and South Atlantic. Using this correction decreases the global inventory of C_{ant} by 7 Pg-C (i.e. without this correction the inventory is 141 Pg-C). As some of the grid boxes with $C_{ant} \leq 2.5$ μmol/kg will actually have non-zero C_{ant} this is probably an over-correction.

4. Uncertainties

As described in Section 2 the TTD method contains several assumptions, and it is important to consider the uncertainties that these introduce into the C_{ant} estimates. In this section we estimate these uncertainties. We first assess the uncertainties due to different assumptions by varying different parameters in the calculations. For example, the uncertainties due to Δ/Γ is estimated by repeating the TTD calculations for different values. However, the impact of some assumptions, for example, assumption of constant disequilibrium, cannot be easily evaluated by varying parameters. We, therefore, use a second approach to assess the accuracy of the method. We apply the TTD method to output from OGCM simulations where the 'true' directly simulated C_{ant} is known. Such an approach was used by Matear et al., (2003) to assess the pCFC age method (for decadal uptake), and by Matsumoto and Gruber (2005) to assess the ΔC^* method. This comparison using synthetic model data allows the combined uncertainties and potential biases to be evaluated.

4.1. *Sensitivity Calculations*

The uncertainty due to assumed Δ/Γ, CFC surface saturation, empirical relationship for Alk^0, and dissociation constants can

be estimated by repeating TTD calculations with different values of these parameters.

As discussed in Section 2 several studies of transient tracers indicate that the TTDs are broad with $\Delta/\Gamma \approx 1$, but there is some uncertainty in the exact value. The thin curves in Fig. 2 show the TTD estimates using Δ/Γ equal to 0.75 and 1.25, rather than 1.0. Consistent with the calculations shown in Fig. 1, there is only very weak sensitivity to Δ/Γ for this range of values. Differences of around 2 μmol/kg are found in the middle and lower depths of North and Tropical Atlantic and Southern Ocean, but smaller differences occur elsewhere. Similar calculations by Waugh et al. (2004) yielded similar results. Waugh et al. (2004) also determined an uncertainty of ± 2 μmol/kg for a 10% uncertainty in the CFC saturation.

Calculations have also been performed to determine the sensitivity of the $C_{ant,0}$ to choice of empirical relationship for Alk^0 and dissociation constants used in the equilibrium chemistry calculations. In both cases there is only weak sensitivity. Using the Alk^0 relationships from Sabine et al. (1999) or Lee et al. (2003) causes a change in Alk^0 of about 20 μmol/kg or less, which introduces an uncertainty in $C_{ant,0}$ of $\pm$ 0.5 μmol/kg. Using different carbonate constants results in a slightly larger variation in $C_{ant,0}$ of ± 1 μmol/kg. These sensitivities are weak because the equilibrium relationship between pCO_2 and DIC is relatively linear over the industrial-era variation in pCO_2. Approximately equal sensitivities to Alk^0 and dissociation rates occur for pre-industrial and industrial times, resulting in little sensitivity in the difference.

Taking the above uncertainties into account we estimate uncertainty of ± 6 μmol/kg for individual estimates of C_{ant}.

4.2. Model-based evaluation

To estimate the combined uncertainties and potential biases in the TTD method, we have applied the TTD method described in Section 2 to the output from the CSIRO GCM (Matear et al., 2003), and compared this TTD-inferred C_{ant} with the 'true' directly simulated C_{ant}.

Figure 4 compares the 'true' model and TTD-inferred vertical profiles of average C_{ant} for the different oceans. There is excellent agreement between the 'true' and inferred distributions in all regions, except the Southern Ocean. Outside the Southern Ocean the 'true' model and TTD-inferred average C_{ant} are nearly always within 1 μmol/kg, the column inventories within 10% (except in equatorial upwelling regions), and the total inventories for the regions shown are within 2 Pg-C (see plot legends). There are, however, larger differences in the Southern Ocean, where the TTD-inferred μmol/kg exceeds the 'true' value by between 2 and 6 μmol/kg. This bias occurs at all depths, but largest differences occur around 500 m. This consistent positive bias causes a large difference in the inventories for the Southern Ocean, with the TTD-inferred Southern Ocean inventory 60% larger than the true value. This bias, together with small bias for rest of the oceans, results in the TTD calculations overestimating the 'true' global inventory by 17%.

The positive bias between TTD-inferred and 'true' C_{ant} is due primarily to the constant disequilibrium assumption. Calculation of the 'saturation' of C_{ant} in the model (i.e. the ratio of surface C_{ant} in the model to that calculated using equilibrium carbon chemistry) is generally between 0.8 and 1.0, but in regions of deep convection (e.g. Weddell Sea, Ross Sea) it is less than 0.5. For an example, see figure 6 of Matear et al. (2003) which shows relative saturation of C_{ant} and CFC12. It is precisely these latter regions where the differences between directly simulated and TTD-inferred C_{ant} are greatest, that is, the largest differences in the Southern Ocean occur 'downstream' of the regions of deep convection in the model. Regions of undersaturation of surface C_{ant} also occur in the tropical eastern Pacific and the TTD overestimates the 'true' C_{ant} in these regions as well. However, this impacts C_{ant} only in the upper few hundred metres and does not have a large impact on the global inventory.

A similar analysis using an off-line version of the MIT global ocean GCM (Khatiwala et al., 2005) produces similar results. The regions and magnitudes of surface undersaturation vary, as do the exact TTD - model differences. However, as with the CSIRO model the regions with large bias appear 'downstream' of regions with large surface undersaturation. Also, the largest differences occur in Southern Oceans, with peak differences around 500–1000 m depth, and the overestimate of global inventory is of similar magnitude (20%).

Given the uncertainties in models and the large spread in model simulations of C_{ant} (e.g. Matsumoto et al., 2004) it is not possible to correct the TTD calculations or to put an exact number of the bias. However, this analysis of two models suggests that the assumption of constant disequilibrium in TTD causes an order 20% overestimate in the global inventory, with the vast majority coming from the Southern Oceans. If we combine this bias with a random uncertainty of around $\pm 10\%$ in the global inventory, due to mapping errors and uncertainty in the CFC measurements, our total uncertainty is -10% to -30%. Adding this to our inventory of 134 Pg-C we obtain an inventory range of 94–121 Pg-C.

5. Comparisons with ¢ C′ Estimates

As discussed in the Introduction, estimates of C_{ant} from the ΔC^* method have received the greatest attention in recent years. We, therefore, compare our new estimates of C_{ant} with the ΔC^* calculations of Sabine et al. (2004). (The ΔC^* estimates used are those on the GLODAP website (http://cdiac.ornl.gov/oceans/glodap/Glodap_home.htm).)

We first compare the ΔC^* estimates with the TTD estimates for the regional averages and column inventories shown earlier, and then examine in more detail the differences for individual samples.

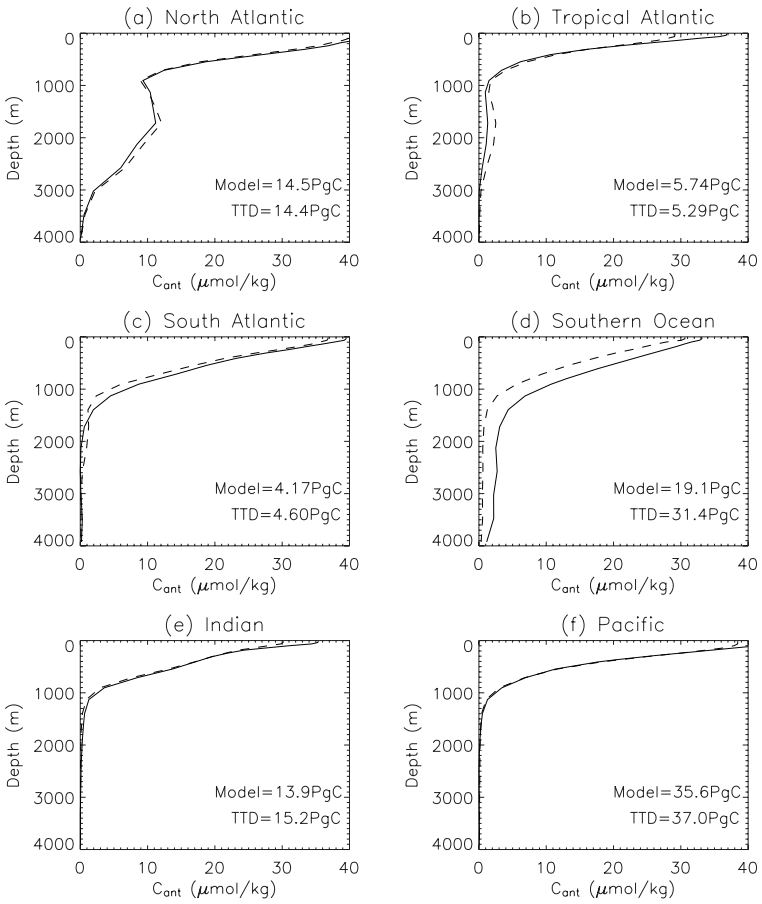

Fig. 4. Comparison of TTD-inferred (solid curves) and 'true' model (dashed) regional-average C_{ant}, from the CSIRO model. Numbers in each plot list the inventories for each region.

5.1. Regional and Global Distributions

The regional-averaged C_{ant} from the Sabine et al. (2004) calculations are shown as the dashed curves in Fig. 2. There is good agreement between the TTD and ΔC^* estimates of the regionally averaged C_{ant} in the upper 1000 m, except in the North Indian Ocean. There is also reasonable agreement below 1000 m in the Indian and Pacific Oceans. However, there are substantial differences below 1000 m in the mean profiles for the Atlantic and Southern Ocean. The sign of these difference varies between locations, but generally C_{ant} from the TTD method is equal to or less than that from ΔC^* in upper and intermediate waters (above 1000 m) and larger in deep waters (below 2000 m). These differences are discussed in more detail below.

The differing sign of the TTD - ΔC^* differences in intermediate and deep waters partially offset when calculating column inventories, but there are still large differences in some regions. Figure 3(b) shows the difference between column inventories from our TTD calculations and Sabine et al. (2004) ΔC^* calculations. In most regions the integrated effect of positive TTD-ΔC^* differences in the deep waters is larger than the negative differences in upper waters, and the TTD estimates of column C_{ant} exceeds that from ΔC^*. Exceptions occur in the North Indian Ocean, high latitude North Pacific, and some tropical Atlantic regions. The difference between the column inventories is less 20 mol/m^2 over most of the globe, but larger differences are found in the Southern Ocean (with differences exceeding 40 mol/m^2 in the Atlantic sector). In the regions with large differences in column C_{ant} the TTD estimates are around 8–10 μmol/kg throughout the water column below 1000 m, whereas the individual ΔC^* estimates are generally near zero or negative (and hence set to zero in inventory calculations) in the same region, for example, Figs. 5(f) and 6(b) below.

Comparison of Table 1 with table S1 of Sabine et al. (2004) shows that there is good agreement between our estimates and the Sabine et al. (2004) estimates of the basin inventories in the tropics and Northern Hemisphere, for example, the TTD inventories for 14–50 N and 14 S to 14 N are only 2 Pg-C larger than the Sabine et al. estimates. However, there are large difference occurs in the Southern Hemisphere: The inventories for 14°–50° S and 70°–50° S are 42 and 10 Pg-C from Sabine et al. (2004) compared with 55 and 21 Pg-C from our calculations. These large Southern Ocean differences result in a smaller total inventory of 106 Pg-C from the ΔC^* calculations compared to the 134 Pg-C from the TTD calculations.

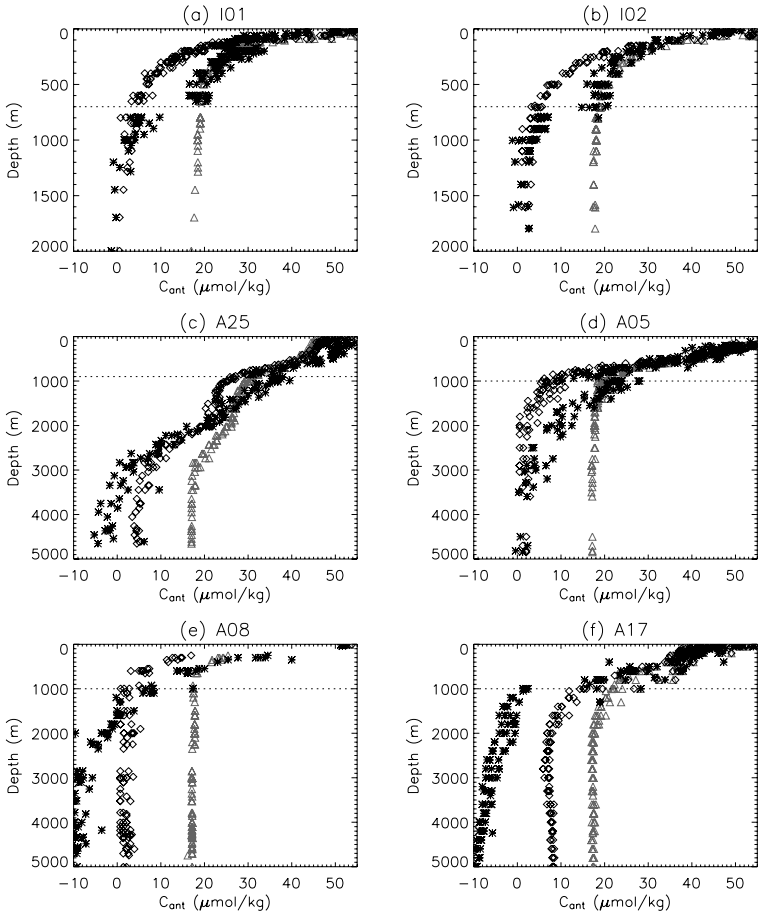

Fig. 5. Vertical profiles of C_{ant} from TTD (diamonds), pCFC age (triangles) and ΔC^* (asterisk) for individual WOCE cruises (a) I01 (Indian Ocean, 7 N), (b) I02 (Indian Ocean, 8 S), (c) A25 (N Atlantic 45–50 N), (d) A05 (N Atlantic, 26 N), (e) A08 (S Atlantic, 11 S) and (f) A17 (S Atlantic, 45 S). Horizontal dotted lines are levels where calculation of disequilibrium in ΔC^* calculations change.

Accounting for the approximate 20% bias in the TTD calculations due to the constant disequilibrium assumption brings the TTD and ΔC^* inventories into agreement. The corrected TTD range is 94–121 Pg-C, and the range of Sabine et al. (2004) is 85–127 Pg-C (106±21 Pg-C). Note, however, that the ΔC^* estimates also suffer from a bias due to the assumption of constant disequilibrium (e.g. Matsumoto and Gruber, 2005), which is not accounted for by Sabine et al. (2004), and which would degrade the TTD-ΔC^* agreement if corrected. In any case, it would be a mistake, to conclude that accounting for the constant-disequilibrium bias brings the underlying C_{ant} distributions into agreement. There are substantial differences in the TTD and ΔC^* distributions of C_{ant} that cannot be explained by this bias. The model calculations indicate little, if any, bias in the TTD calculations outside the Southern Ocean, while there are TTD-ΔC^* differences throughout the major basins.

5.2. Detailed Comparisons

We now examine in more detail the C_{ant} estimates, focusing on regions where there are large differences between the TTD and ΔC^* estimates. Figures 5 and 6 compare the TTD (diamonds), pCFC age (triangles), and ΔC^* (asterisk) estimates for individual measurements made on several cruises. For clarity, we only plot data from relatively short portions of each cruise. Below we examine the TTD-ΔC^* differences in each of the ocean basins shown.

5.2.1. Indian Ocean. Figure 2(e) shows that there is a large difference between the ΔC^* and TTD estimates in the northern Indian Ocean for depths between 200 and 1000 m. This difference is clearly seen in the calculations for individual cruises. For example, Figs. 5(a) and (b) show estimates of C_{ant} from the near-zonal cruises in the northern and southern Indian Ocean. Above 700 m the ΔC^* estimate is similar to the pCFC age estimate whereas below this ΔC^* is similar to the TTD estimate. Furthermore, there is a sharp drop (discontinuity) in the ΔC^* estimate of around 10 μmol/kg at 700 m for both cruises. Such sharp drops in ΔC^* are also found in other regions.

The change in the ΔC^* estimates above and below 700 m appears to be related to the determination of the air–sea disequilibrium of CO_2, ΔC_{diseq}, in the ΔC^* calculations. In the ΔC^* method the air–sea disequilibrium is estimated two ways. On deep isopycnals where there is a region remote from the source that is thought to be free of anthropogenic CO_2 ('uncontaminated' surfaces) the measured values in this region are used to determine ΔC_{diseq}. On isopycnals where no such regions exist

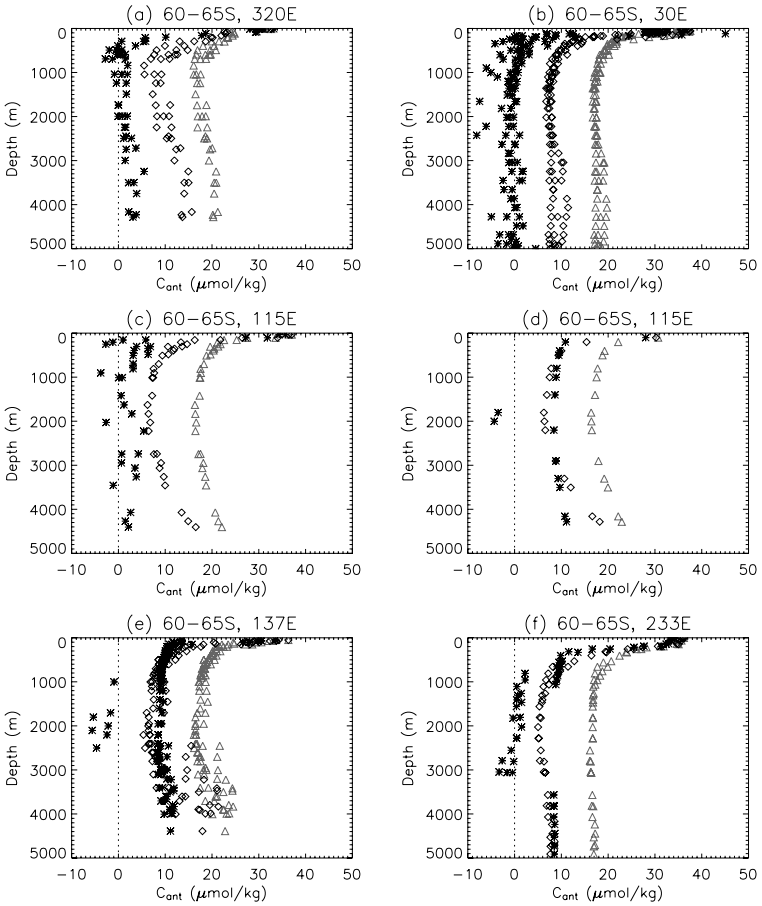

Fig. 6. Vertical profiles of C_{ant} for different longitudes in the Southern Ocean (60–70 S). Panels (c) and (d) show the same longitude but from two different cruises.

('fully contaminated' surfaces) ΔC_{diseq} is assumed constant in time (but not space) and is calculated by comparing the measured DIC with a biological correction removed (C_{obs} - C_{bio}) with the DIC in equilibrium with the atmosphere τ years earlier, where τ is the water mass age. All ΔC_{diseq} for water with τ less then a threshold (25 or 30 yr) are averaged. In the Sabine et al. (1999) analysis the ΔC^* calculations changes from 'fully contaminated' and 'uncontaminated' method at $\sigma_\theta = 27.25$, which is the level of the discontinuity shown in Figs. 5(a) and (b). Furthermore, the change in ΔC^* at this depth equals the change in ΔC_{diseq} at $\sigma_\theta = 27.25$, as shown in Tables 2 and 3 of Sabine et al. (1999). We conclude that the discontinuity in C_{ant} is an artefact of the ΔC^* method.

The procedure for estimating ΔC_{diseq} on the 'fully contaminated' surfaces assumes that the CFC is a good proxy for C_{ant}, which would be the case if either (1) the two tracers had the same atmospheric history or (2) if each interior parcel was dominated by a unique ventilation time. Neither is true, however, and the resulting ΔC_{diseq} and C_{ant} are overestimated (Hall et al., 2002; Matsumoto and Gruber, 2004). In fact, in the 'short cut' version of the ΔC^* method (Gruber et al., 1996) use of CFC in this manor is equivalent to computing C_{ant} directly by lagging the anthropogenic DIC time-series at the outcrop with τ_{CFC}, which is identical to the TTD approach with $\Delta/\Gamma = 0$ (Hall et al., 2002; Waugh et al., 2003). Computing C_{ant} in this way where τ_{CFC} is small incurs only small error, but values computed where τ_{CFC} is large are large overestimates, as seen in Fig. 2. In the implementation of ΔC^* used by Sabine et al. (2002) ΔC_{diseq} is computed and averaged only for water with $\tau_{CFC} \leq 25$ yr, which buffers the calculation from the most extreme biases. Nevertheless, Waugh et al. (2003) has shown that even when τ_{CFC} is as low as 20 yr it differ significantly from a tracer age derived from a hypothetical tracer with a time history matching anthropogenic DIC.

The differences between TTD and ΔC^* estimates in the upper 700 m are consistent with the different assumptions regarding transport in the methods. By assuming that a single transit time dominates the ventilation of water parcels, the ΔC^* estimates of C_{ant} are larger than the TTD estimates, which utilize a wide range of ventilation times. This alone does not indicate which estimates are more realistic, because we have not established the range of ventilation time scales. However, examination of the relationship between CFC11 and CFC12 measurements in the Indian Ocean indicates that the TTDs are broad (Hall et al., 2004), and hence the assumption of a single ventilation time in the ΔC^* and pCFC age methods is suspect. Because of this we expect the TTD estimates to be more realistic. Further support

for the TTD estimates comes from comparisons with estimates using the MIX method of Goyet et al. (1999). Even though TTD and MIX methods are very different, the estimates of C_{ant} for the WOCE I01 line compare reasonably well. Both the TTD and MIX estimates show much lower C_{ant} than ΔC^* in the upper 700 m. For example, compare Fig. 5(a) with figure 1 of Coatanoan et al. (2001).

5.2.2. North Atlantic Ocean. Figs. 5(c,d) compare estimates of C_{ant} for the WOCE A25 ($\sim$47° N) and A05 ($\sim$26° N) cruises in the North Atlantic Ocean. The ΔC^* and TTD estimates generally agree in the upper 700 m, where there is no sensitivity to mixing (i.e. pCFC age and TTD estimates agree). However, below this level there are differences between the methods, with the exact differences varying with location.

The TTDs between 1000 and 2000 m in the North Atlantic are well constrained by transient tracer measurements, and can be well modelled by inverse Gaussian with $\Delta = \Gamma$ (Waugh et al., 2004). Hence within this region we have confidence that our assumption regarding the TTDs is valid. Between 1000 and 2000 m the ΔC^* estimate is generally higher than the TTD estimate. As discussed above this difference in 'fully contaminated' isopycnals is consistent with the assumption of weak mixing of water of different ages used in the calculation of the disequilibrium ΔC_{diseq} term in the ΔC^* method. Lee et al. (2003) considered several different water mass sources and used a optimum multiparameter (OMP) analysis to determine ΔC_{diseq} of a given measurement. However, this OMP analysis does not account for each water-mass component having a range of transit times since ventilation. For isopycnals shallower than $\sigma_\theta = 27.5$ (1000 m) the 'fully contaminated' method is used to calculate ΔC_{diseq} for all water masses, but for deeper surfaces the method varies between the contaminated and uncontaminated methods depending on the water mass. However, the water around 1000 m shown in Figs. 5(c) and (d) is primarily North Atlantic Central Water (NACW) which is determined using the contaminated method both above and below $\sigma_\theta = 27.5$. Hence, the fact that the C_{ant} estimates are larger than those of of the TTD is consistent with the expected bias due to the assumption of a single ventilation time for parcels in ΔC^*.

The difference in C_{ant} below 3000 m between the ΔC^* and TTD estimates is generally the reverse of that between 1000 and 2000 m. As Lee et al. (2003) used the 'uncontaminated' method to estimate ΔC_{diseq} on these deep isopycnals, this is again consistent with the bias in the ΔC^* method. On uncontaminated surfaces there is a region where CFC concentrations are below the detection threshold and the measured DIC is assumed to equal the pre-industrial DIC. However, as CFCs have a much short atmospheric history than C_{ant} it is possible that mixing has transported water with industrial-era DIC, but no CFCs, into this region. This would mean that the pre-industrial DIC and ΔC_{diseq} are overestimated and C_{ant} underestimated.

Closer inspection of Figs. 5(c) and (d) shows that there are again discontinuities in the ΔC^* estimates. These discontinuities occur at $\sigma_\theta = 27.5$ (around 1000 m), with C_{ant} from ΔC^* around 6 to 7 μmol/kg higher just above $\sigma_\theta = 27.5$ than below it. As with the Indian Ocean calculations, the level with the jump in C_{ant} is a level of transition in the ΔC_{diseq} calculation. As discussed above, Lee et al. (2003) performed separate OMP analyses above and below $\sigma_\theta = 27.5$, so it is not straightforward to relate changes in C_{ant} to changes in ΔC_{diseq}. However, the ΔC_{diseq} for NACW with density greater than 27.5 is larger than that for less dense water masses (see table 2 of Lee et al., 2003), consistent with the sign of the jump in C_{ant}. The discontinuities in the ΔC^* estimates of C_{ant} may again be an artefact of the ΔC^* method.

5.2.3. South Atlantic Ocean. The comparisons between TTD and ΔC^* estimates for the South Atlantic are similar to that for the North Atlantic: The two estimates agree in upper waters, the ΔC^* estimate is larger in intermediate waters (500–1000 m), and the TTD estimate is larger in deep waters, for example, Figs. 5(e) and (f). There is also a discontinuity in the ΔC^* estimates of C_{ant} at $\sigma_\theta = 27.5$ ($\sim$1000 m) that is consistent with change in ΔC_{diseq}. In this case the water mass is Antarctic Intermediate Water (AAIW) and the change in ΔC_{diseq} above and below $\sigma_\theta = 27.5$ is around 10 μmol/kg .

A striking feature of the ΔC^* estimates for the tropical and Southern Atlantic is the large negative values (around -5 to -10 μmol/kg) in C_{ant} for some deep water locations, see Figs. 5(e) and (f). The cause of these negative values is unknown but is presumably related to uncertainties in the ΔC^* method, and indicates that the uncertainty in the ΔC^* estimates from Lee et al. (2003) is at least 10 μmol/kg. Note that large negative values are not found in the calculations of C_{ant} in the same region by Gruber (1998). This suggests that the negative values may be an implementation issue. Sabine et al. (2004) set any negative values to zero when computing the inventory, but one might reasonably be concerned whether features of the analysis leading to erroneous negative values leak into small positive values.

5.3. Southern Ocean

Finally we consider the differences between the TTD and ΔC^* estimates in the Southern Ocean. There is a large difference between the zonal mean C_{ant} from the two methods (Fig. 2d). As discussed earlier there is the potential for a significant bias in the TTD estimates in the Southern Ocean, and this likely contributes to the differences. However, there may be other causes as well.

The characteristics of the differences vary with longitude. This is shown in Fig. 6 which compares the estimates of C_{ant} in the Southern Ocean (60°–70° S) for several different longitudes. There is good agreement between the TTD and ΔC^* estimates in the upper 500 m, where both methods assume constant disequilibrium. There are however, differences below 500 m. There are only weak longitudinal variations in the TTD estimates below 500 m, but the ΔC^* estimates have a large longitudinal variation with values as high as 10 μmol/kg (which generally agree with the TTD values) in the Pacific sector (120°–270° E) and

much lower values around 0 μmol/kg in the Indian and Atlantic sectors.

Before considering this longitudinal variation in more detail we note that there are again discontinuities in vertical profiles from the ΔC^* method, for example, Figs. 6(d)–(f). These occur only for cruises in the Pacific Ocean, and again appear to be related to a change in the method used to estimate the disequilibrium term. The C_{ant} drops from $\sim$10 to $\sim$0 μmol/kg when the CFC11 age increases just above 35 yrs (CFC11 concentration drops below 0.15 pmol/kg). We suspect this is due to the calculation of ΔC_{diseq} switching from the contaminated to uncontaminated method. [Sabine et al. (2002) state that they switched from the contaminated to uncontaminated methods when the CFC age equalled 30 yrs, but the data suggest that 35 yrs was used.] As a very small change in CFC concentration at these low levels results in a large decrease in the ΔC^* estimates of C_{ant} the longitude variation in C_{ant} in the Pacific Ocean sector of Southern Ocean (e.g. figure 7 of Sabine et al., 1999) is most likely an artefact of the implementation of the ΔC^* method.

Such spurious discontinuities do not, however, explain the TTD-ΔC^* differences in C_{ant} between the Pacific sector and the Indian or Atlantic sectors, as these differences occur above the discontinuities. For example, at 500 m the ΔC^* estimates are around 10 μmol/kg throughout the Pacific sector, but near zero in the Indian and Atlantic sectors. The cause of the differences between sectors is not known. The fact that the ΔC^* method was applied differently in the three sectors suggests that the differences may be due to different implementations of the ΔC^* method, rather than real geophysical differences. It would be of interest to apply the ΔC^* method uniformly to the Southern Ocean data.

Although the above discontinuities and differences between sectors casts doubt on the reality of the longitudinal variations in the ΔC^* estimates, it is important to note that the positive bias in the TTD method may vary with longitude. The degree of undersaturation of surface C_{ant} related to that of CFC12 could, and likely does, vary with longitude, and so we would expect the bias to also vary with longitude, that is, larger bias downstream of regions with lower saturations. This is seen in the models considered in Section 3, although the magnitude is small and the spatial variation is not consistent with that seen in the ΔC^* estimates.

At the same time there could be a negative bias in ΔC^* estimates due to the undersaturation of oxygen, which is thought to also occur in the above deep-water formation regions. If the surface oxygen is undersaturated then calculations of the biological correction in the ΔC^* method will be overestimated (if surface saturation is assumed), which results in an underestimate of C_{ant}. LoMonaco et al. (2005a) showed that this can cause biases as large as 10 μmol/kg in the Southern Ocean. Note that Matsumoto and Gruber (2005) claim that this error cancels out in the calculation of C_{ant} as an error of the opposite sign is made in the ΔC_{diseq} calculation. However, while there will be some cancellation it is not necessarily complete as the ΔC^* values are derived for each sample location whereas the ΔC_{diseq} is an average over a number of observations at a similar density.

6. Conclusions

This study has presented new global estimates of anthropogenic carbon (C_{ant}) in the oceans using the TTD method.[1] Unlike most other inference methods, the TTD method does not assume a single ventilation time and avoids the large uncertainty incurred by attempts to correct for the large natural carbon background in DIC measurement. Furthermore, as only measurements of temperature, salinity and CFC12 are required, the TTD method is easily applied. Finally, it can be used to infer the time evolution of C_{ant} (Hall et al., 2004), although we have not done that here. The highest concentrations and deepest penetration of C_{ant} in the new estimates occur in the North Atlantic and Southern Oceans (C_{ant} $\sim$ 8 μmol/kg at 5000 m depth and column inventories exceeding 60 mol/m^2), and the uncorrected estimated total inventory for the GLODAP data is 134 Pg-C which corresponds to a global inventory around 146 Pg-C when marginal seas are included.

A model-based assessment of the TTD method indicates that it is accurate to within 1 μmol/kg outside the Southern Ocean, but that the assumption of constant disequilibrium in TTD likely causes a large positive bias in the Southern Ocean. The model analysis indicates this bias results an order 20% overestimate in the global inventory. Accounting for this bias and other centred uncertainties, we obtain an inventory range of 94–121 Pg-C for the GLODAP data. This agrees with the inventory of Sabine et al. (2004), who applied the ΔC^* method to the same data.

Although the total inventories from our TTD calculations and the Sabine et al. (2004) ΔC^* calculations are in agreement, there are significant differences in the C_{ant} distributions. The TTD and ΔC^* estimates generally agree in upper waters, but differences are found in intermediate and deep waters. The TTD estimates are generally smaller than ΔC^* estimates in intermediate waters but larger in deep waters. In most cases the sign of the differences between the two estimates are consistent with the differences in the treatment of transport in the methods. In the TTD calculations we have assumed a broad TTDs, which is supported by analyses of tracers (Robbins et al., 2000; Hall et al., 2004; Mecking et al., 2004; Waugh et al., 2004). In contrast, the ΔC^* calculations assumes a single transport (ventilation) time, which can lead to an overestimate of C_{ant} on isopycnals that are assumed to be 'fully contaminated' and an underestimate on deep 'uncontaminated' isopycnals (Hall et al., 2002; Matsumoto and Gruber, 2005). The tendency for the ΔC^* estimates to exceed the TTD estimates on intermediate levels but to be smaller on deep levels is consistent with these biases.

[1]These estimates will be added to the next release of the GLODAP data set.

Given the uncertainties in both the TTD and ΔC^* estimates it is clear that more research is needed before we can be confident of our knowledge of the ocean carbon uptake. Particular attention is required for the Southern Ocean. This region is very important for understanding and predicting future climate change, all inference methods (not only the two considered here) have larger uncertainties in this region, and there is large discrepancies among ocean models.

7. Acknowledgments

This work was supported by NOAA grant NA04OAR4310118 and NSF grant OCE-0437888.

References

Brewer, P. G. 1978. Direct observation of the oceanic CO2 increase. *Geophys. Res. Lett.* **5**, 997–1000.

Brewer, P. G., Bradshaw, A. L., Shafer, D. K. and Williams, R. T. 1986. Measurements of total carbon dioxide and alkalinity in the North Atlantic Ocean in 1981. In: *The Changing Carbon Cycle: A Global Analysis*, (eds. J. R. Trabalka and D. E. Reichle), Springer, New York, 348–370.

Millero, F. J. 1979. Gradual increase of oceanic CO_2. *Nature* **277**, 205–206.

Coatanoan, C., Goyet, C., Sabine, C. L. and Warner, M. 2001. Comparison of the two approaches to quantify anthropogenic CO_2 in the ocean: results from the northern Indian. *Global Biogeochem. Cycles* **15**, 11–26.

Dickson, A.G. and Millero, F.J. 1987. A comparison of the equilibrium constants for the dissocaition of carbonic acid in seawater media. *Deep-Sea Res.* **40A**, 107–118.

Friis, K., Kortzinger, A., Patsch, J. and Wallace, D. W. R. 2005. On the temporal increase in anthropogenic CO_2 in the subpolar North Atlantic. *Deep-Sea Res.* **52**, 681–698.

Gloor, M., Gruber, N., Sarmiento, J., Sabine, C.L., Feely, R. A., and co-authors. 2003. A first estimate of present and preindustrial air-sea CO_2 flux patterns based on ocean interior carbon measurements and models. *Geophys. Res. Lett.* **30**, doi:10.1029/2002GL015594.

Goyet, C., Coatanoan, C., Eischeid, G., Amaoka, T., Okuda, K., and co-authors 1999. Spatial variation of total CO2 and total alkalinity in the northern Indian Ocean: a novel approach for the quantification of anthropogenic CO_2 in seawater. *J. Marine Res.* **57**, 135–163.

Gruber, N., 1999. Anthropogenic CO_2 in the Atlantic Ocean. *Global Biogeochem. Cycles* **12**, 165–191.

Gruber, N., Sarmiento, J. L. and Stocker, T.F., 1996. An improved method for detecting anthropogenic CO_2 in the oceans. *Global Biogeochem. Cycles* **10**, 809–837.

Haine, T. W. N. and, Hall, T. M. 2002. A generalized transport theory: water-mass composition and age, *J. Phys. Oceanogr.* **32**, 1932–1946.

Hall, T. M., Haine, T. W. N. and Waugh, D. W. 2002. Inferring the concentration of anthropogenic carbon in the ocean from tracers. *Global Biogeochem. Cycles* **16**, doi:10.1029/2001GB001835.

Hall, T. M., Waugh, D. W., Haine, T. W. N., Robbins, P. E. and Khaliwala, S. 2004. Reduced estimates of anthropogenic carbon in the Indian Ocean due to mixing and time-varying air-sea CO_2 diseqilibrium. *Global Biogeochem. Cycles* **18**, doi:10.1029/2003GB002120.

Hall, T. M. and Plumb, R. A. 1994. Age as a diagnostic of stratospheric transport. *J. Geophys. Res.*, **99**, 1059–1070.

Houghton, J. T., Ding Y., Griggs, D. J., Noguer, M., van der Linden, P. J., and co-authors, 2001. Climate Change 2001: The Scientific Basis. Cambridge University Press, Cambridge, 881.

Khatiwala S., Visbeck M. and Cane M. A. 2005. Accelerated simulation of passive tracers in ocean circulation models. *Ocean Modelling* **9**, 51–69.

Keeling, R. F. 2005. Comment on 'The Ocean Sink for Anthropogenic CO_2'. *Science* **308**, 1743.

Key, R. M., Kozyer A., Sabine, C. L., Lee, K., Wanninkhof, R., and co-authors, 2004. A global ocean carbon climatology: results from Global Data Analysis Project (GLODAP). *Global Biogeochem. Cycles* **18**, doi:10.1029/2004GB002247.

Lee, K., Choi, S. D., Park, G. H., Wanninkhof, R., Peng T. H., and co-authors, 2003. An updated anthropogenic CO_2 inventory in the Atlantic Ocean. *Global Biogeochem. Cycles* **17**, doi:10.1029/2003GB002067.

Lo Monaco C., Metzl, N., Poisson, A., Brunet C., and Schauer, B. 2005a. Anthropogenic CO2 in the Southern Ocean : distribution and inventory at the Indo-Atlantic boudary (WOCE line I6). *J. Geophys. Res.* **110**, doi:10.1029/2004JC002643.

Lo Monaco C., Goyet, C., Metzl, N., Poisson, A. and Touratier F. 2005b. Distribution and inventory of anthropogenic CO_2 in the Southern Ocean: comparison of three data-based methods. *J. Geophys. Res.* **110**, doi:10.1029/2004JC002571.

Matear, R. J., C. S. Wong and L. Xie, 2003. Can CFCs be used to determine anthropogenic CO_2. *Global Biogeochem. Cycles* **17**, doi:10.1029/2001GB001415.

Matsumoto, K., Sarmiento J. L., Key, R. M., Aumont, O., Bullister, J. K., and co-authors 2004. Evaluation of ocean carbon cycle models with data-based metrics. *Geophys. Res. Lett.* **31**, doi:10.1029/2003GL018970.

Matsumoto, K. and Gruber, N. 2005. How accurate is the estimation of anthropogenic carbon in the ocean? An evaluation of the ΔC^* method. *Global Biogeochem. Cycles* **19**, doi:10.1029/2004GB002397.

McNeil B. I., Matear, R. J., Key, R. M., Bullister J. L., and Sarmiento, J. L., 2003. Anthropogenic CO_2 uptake by the ocean based on the global chlorofluorocarbon data set. *Science* **299**, 235–239.

Mecking S., Warner M. J., Greene C. E., Hautala S. L. and Sonnerup R. E. 2004. Influence of mixing on CFC uptake and CFC ages in the North Pacific thermocline. *J. Geophys. Res.* **109**, doi: 10.1029/2003JC001988.

Merbach, C., Culberson, C. H., Hawley, J. E. and Pytkowicz, R. M. 1973. Measurements of the apparent dissociation constants of carbonic acid in seawater at atmospheric pressure. *Limnology and Oceanography* **18**, 897–907.

Mikaloff-Fletcher, S. E., Gruber, N., Jacobson, A. R., Doney, S. C., Dutkiewicz, S., and co-authors. 2006, Inverse estimates of anthropogenic carbon uptake, transport, and storage by the ocean. *Global Biogeochem. Cycles*, **20**, doi:10.1029/2005GB002530

Orr, J. C., Maier-Reimer, E., Mikolajewicz, U., Monfray, P., Sarmiento, J. L., and co-authors. 2001. Estimates of anthropogenic carbon uptake from four three-dimensional global ocean models. *Global Biogeochem. Cycles* **15**, 43–60.

Robbins, P. E., Price J. F., Owens, W. B. and Jenkins W. J. 2000. On the importance of lateral diffusion for the ventilation of the lower thermocline in the subtropical North Atlantic. *J. Phys. Oceanogr.* **30**, 67–89.

Sabine, C. L. and Feely, R. A. 2001. Comparison of recent Indian Ocean anthropogenic CO_2 estimates with a historical approach. *Global Biogeochem. Cycles* **15**, 31–42.

Sabine, C. L. and Gruber, N. 2005. Response to Comment on "The Ocean Sink for Anthropogenic CO_2". *Science* **308**, 1743.

Sabine, C. L., Key, R. M., Johnson K. M., Millero, F. J., Poisson, A., and co-authors. 1999. Anthropogenic CO_2 inventory of the Indian Ocean. *Global Biogeochem. Cycles* **13**, 179–198.

Sabine, C. L., Feely, R. A., Key, R. M., Bullister, J. L., Millero, F. J., and co-authors. 2002. Distribution of anthropogenic CO_2 in the Pacific. *Global Biogeochem. Cycles* **16**, doi:10.1029/2001GB001639.

Sabine, C. L., Feely, R. A., Gruber, N., Key, R. M., Lee, K., and co-authors. 2004. The Oceanic Sink for Atmospheric Carbon. *Science* **305**, 367–371.

Thomas, H. and Ittekkot, V., 2001. Determination of anthropogenic CO_2 in the North Atlantic Ocean using water mass ages and CO_2 equilibrium chemistry. *Journal of Marine Systems* **27**, 325–336.

Touratier F. and Goyet, C. 2004. Applying the new TrOCA approach to assess the distribution of anthropogenic CO_2 in the Atlantic Ocean. *Journal of Marine Systems* **46**, 181–197.

Walker, S. J., Weiss, R. F. and Salameh, P. K. 2000. Reconstructed histories of the annual mean atmospheric mole fractions for the halocarbons CFC-11, CFC-12, CFC-113, and carbon tetrachloride. *J. Geophys. Res.* **105**, 14 285–14 296.

Wallace, D. W. R. 1995. Monitoring global ocean carbon inventories. Ocean Observing System Development panel. Texas A & M University, College Station, Texas, 54.

Wanninkhof, R., Doney, S. C., Peng, T. H., Bullister, J. L., Lee, K. and Feely, R. A. 1999. Comparison of methods to determine the anthropogenic CO_2 invasion into the Atlantic Ocean. *Tellus* **51B**, 511–530.

Waugh, D. W., Haine, T. W. N. and Hall, T. M., 2004. Transport times and anthropogenic carbon in the subpolar North Atlantic Ocean. *Deep-Sea Res.* **51**, 1475–1491.

Waugh, D. W., Hall, T. M. and Haine, T. W. N. 2003. Relationships among Tracer Ages. *J. Geophys. Res.* **108**, doi:10.1029/2002JC001325.

Waugh, D. W., Vollmer M. K., Weiss, R. F., Haine T. W. N. and Hall, T. M. 2002. Transit time distributions in Lake Issyk-Kul. *Geophys. Res. Lett.* **29**, doi:10.1029/2002GL016201.